

On the Fermi level pinning in as-grown GaInNAs(Sb)/GaAs quantum wells with indium content of 8%–32%

R. Kudrawiec,^{1,a)} H. B. Yuen,¹ S. R. Bank,¹ H. P. Bae,¹ M. A. Wistey,¹ James S. Harris,¹ M. Motyka,² and J. Misiewicz²

¹*Solid State and Photonics Laboratory, Department of Electrical Engineering, 311X CISX, Via Ortega, Stanford University, Stanford, California 94305-4075, USA*

²*Institute of Physics, Wrocław University of Technology, Wybrzeże Wyspińskiego 27, 50-370 Wrocław, Poland*

(Received 24 March 2008; accepted 22 May 2008; published online 8 August 2008)

Modified van Hoof structures containing GaInNAs(Sb) quantum wells (QWs) with indium content varying from 8% to 32% have been investigated using contactless electroreflectance (CER) spectroscopy. In CER spectra, both the QW transitions and GaAs-related Franz–Keldysh oscillations (FKOs) have been clearly observed. The band gap discontinuity at the GaInNAs(Sb)/GaAs interface has been determined by analyzing the QW transitions. The built-in electric field in the GaAs cap layer has been extracted from the FKO periodicity. The Fermi level position in the GaInNAs(Sb) QW has been determined through knowledge of the electric field in the GaAs cap layer and band gap discontinuity in the GaInNAs(Sb)/GaAs QW. It has been found that the Fermi level is pinned for all samples at the same energy, ~ 4.7 eV below the vacuum level. The Fermi level is located very close to the Fermi level stabilization energy, ~ 4.9 eV below the vacuum level. A high concentration of native point defects in the as-grown material is the reason for the Fermi level pinning at this energy.

© 2008 American Institute of Physics. [DOI: 10.1063/1.2961330]

I. INTRODUCTION

III-N_x-V_{1-x} alloys ($x < 0.05$) belong to the class of highly mismatched semiconductor alloys. Small quantities of highly electronegative elements (N atoms) replace metallic anions (As, Sb, or P atoms) and cause dramatic changes in the band structure^{1–5} and optical properties of the host. The most important properties of III-N_x-V_{1-x} alloys, otherwise known as dilute nitrides, are a large reduction in the fundamental band gap energy (100–150 meV/% of nitrogen)⁶ and a significant increase in the electron effective mass.^{7,8} Another feature typically observed with dilute nitrides is the deterioration of the structural and optical properties of the III-V host due to the incorporation of nitrogen atoms. It has been found that the N-related damage is enhanced when the indium and nitrogen concentrations in GaInNAs are increased to extend the emission wavelength of GaInNAs/GaAs quantum wells (QWs) to 1.55 μm .⁹ Most as-grown materials exhibit poor photoluminescence (PL), or even lack of it, at room temperature, confirming a high concentration of native defects such as vacancies and interstitials. These defects can pin the Fermi level in undoped materials at specific characteristic energies for these defects. Recently, we have proposed a simple approach to determine the Fermi level position in the QW region.¹⁰ In addition, it has been observed that the Fermi level in GaInNAs/GaAs QWs is pinned at a characteristic energy, but the nature of this pinning has not been explained.¹⁰ The aim of this paper is to investigate the nature of the Fermi position in as-grown GaInNAs(Sb)/GaAs QWs with indium content of 8%–32% and perfect planar morphology. For Sb-free QWs with high

In content, it is difficult to control the growth morphology,^{11–13} and therefore in addition to point defects, extended defects can appear for In-rich GaInNAs/GaAs QWs. These extended defects can influence the Fermi level position separately, and therefore a discussion on the nature of the Fermi level pinning in QWs with these extended defects can be more difficult and complex. The addition of antimony as a surfactant improves the growth conditions, facilitates two-dimensional growth, and eliminates the extended defects.¹³ For perfect planar GaInNAsSb/GaAs QWs, the Fermi level pinning will be associated with native point defects only. Many of them can be removed from GaInNAsSb by postgrowth annealing. Currently, this process is a standard step in laser fabrication. However, the ability to improve the material quality by annealing is limited. It is impossible to achieve a high quality material by annealing poor as-grown samples. Therefore, the quality of as-grown material should be as good as possible. In this work the Fermi level position is investigated for GaInNAsSb grown under optimal growth conditions.^{13–16} For these growth conditions and an optimal anneal, we have obtained GaInNAsSb lasers emitting at 1.5 μm , with the lowest threshold current reported for dilute nitride lasers in this spectral range to date.¹⁶ However, it should be noted that such good laser performances would be impossible to achieve without the annealing process. There remains an issue with the quality of as-grown dilute nitrides. Note that this issue seems to be addressed to the applied physics, but the understanding of defect formation in a given material system is a fundamental problem of the solid state physics. Since the formation energy of native point defects varies with the Fermi energy,¹⁷ an experimental investigation of the Fermi level position in dilute nitrides is important. This paper addresses this prob-

^{a)}Electronic mail: kudrawiec@snow.stanford.edu.

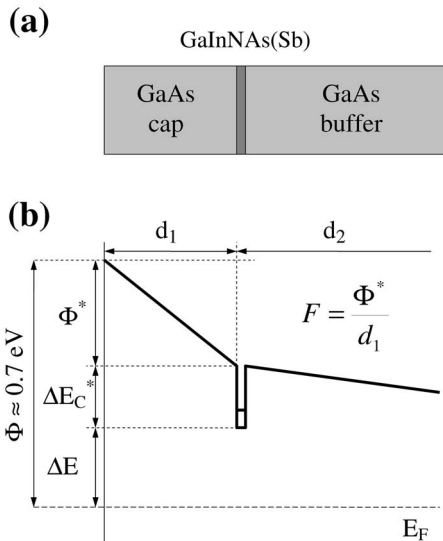


FIG. 1. (a) Layer sequence and (b) band bending in the modified van Hoof structure containing a GaInNAs(Sb) QW.

lem and shows that the Fermi level is pinned very close to the Fermi level stabilization energy E_{FS} for the as-grown GaInNAs(Sb) material, whereas for N-free III-V semiconductors (GaAs, InP, GaSb, etc.), the Fermi level is located in the middle of the energy gap; i.e., it is not correlated with the E_{FS} .

In order to measure the Fermi position in GaInNAsSb QWs, we have applied an experimental approach, which was proposed in Ref. 10. This approach utilizes contactless electroreflectance (CER) spectroscopy and a very simple design of semiconductor structures. The idea of this design is to insert a GaInNAs(Sb) QW into a region of undoped GaAs layer grown on a *n*-type GaAs substrate (see Fig. 1). The possible pinning of the Fermi level in GaInNAs(Sb) material modifies band bending in this system. In CER spectra, both QW transitions and GaAs-related Franz–Keldysh oscillations (FKOs) are clearly observed. The analysis of QW transitions allows us to determine the band gap discontinuity at the GaInNAsSb/GaAs interface, whereas the analysis of FKOs allows us to determine the built-in electric field in the GaAs cap layer. Finally, we are able to find the Fermi level position in the GaInNAs(Sb) QW region.¹⁰

II. EXPERIMENTAL DETAILS

The GaInNAsSb/GaAs QW samples used in this study were grown on *n*-type (100) GaAs substrates by solid-source molecular beam epitaxy (MBE) in a Varian Mod Gen-II system. Gallium and indium were supplied by Veeco SUMO® effusion cells. A valved arsenic cracker supplied As_2 , and an unvalved antimony cracker supplied monomeric antimony. Different indium compositions were obtained by changing the ratio of indium and gallium fluxes. Nitrogen was supplied by a modified SVT Associates plasma cell operating at a rf of 13.56 MHz. Nitrogen concentration in all samples was constant at 2.5%. The GaAs buffer and cap layers were grown at a 580 °C temperature. Other relevant details of MBE growth are described elsewhere.¹⁴ The structure for all samples consists of a 7.5 nm GaInNAsSb QW grown on a

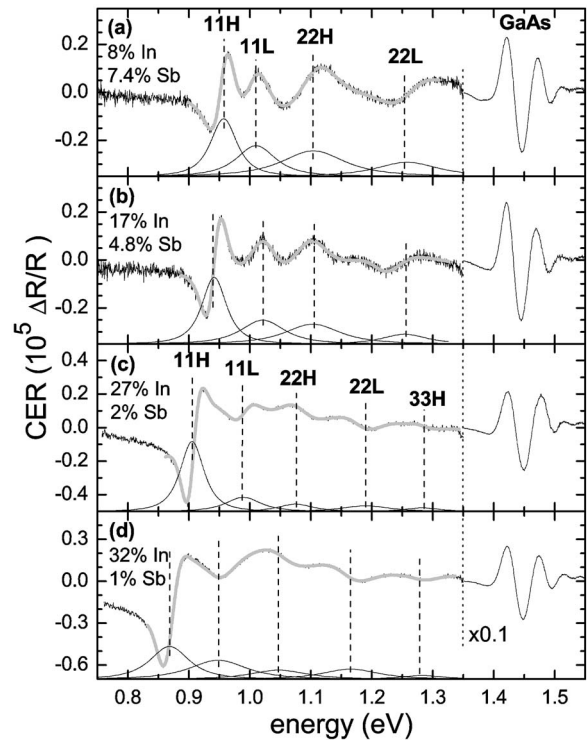


FIG. 2. Room temperature CER spectra for modified van Hoof structures with (a) $Ga_{0.92}In_{0.08}N_{0.025}As_{0.901}Sb_{0.074}$, (b) $Ga_{0.83}In_{0.17}N_{0.025}As_{0.927}Sb_{0.048}$, (c) $Ga_{0.73}In_{0.27}N_{0.025}As_{0.955}Sb_{0.02}$, and (d) $Ga_{0.68}In_{0.32}N_{0.025}As_{0.965}Sb_{0.01}$ QWs.

300 nm GaAs buffer and capped by a 50 nm GaAs layer. From cross section transmission electron microscopy measurements, which were performed for other QWs,¹⁵ it is known that at these growth conditions the QWs have smooth interfaces. The composition of the samples was determined by a high-resolution x-ray diffraction and a secondary-ion mass spectrometry.¹⁴ It was observed that all the samples have well defined QW signals and strong Pendellösung fringes, indicating good structural quality (see Ref. 14).

In addition, two Sb-free QWs with $\sim 2.5\%$ N, and low (10%) and high (32%) indium contents are analyzed in this paper. The samples were grown in the same growth conditions as Sb-containing QWs.¹⁴ In the case of the GaInNAs/GaAs QW with high indium content, some extended defects are possible since this sample exhibited very poor optical quality even after annealing (see appropriate PL spectra in Ref. 14). In addition, it is known that the growth window for Sb-free planar QW growth is expected at ~ 380 °C,^{11,12} whereas this QW was grown at 440 °C. For remaining Sb-free QWs, native point defects are only expected since these QWs were grown in the two-dimensional mode.^{13,15}

In order to measure CER spectra, a so-called bright configuration of the setup has been used.¹⁸ Relevant details of CER measurements are described in detail elsewhere.^{19–21} In order to eliminate a possible photovoltaic effect, the GaAs-related FKOs have been measured in dark configuration by utilizing another experimental setup, which was described in Ref. 22.

III. RESULTS AND DISCUSSION

Figure 2 shows CER spectra for GaInNAsSb/GaAs QWs

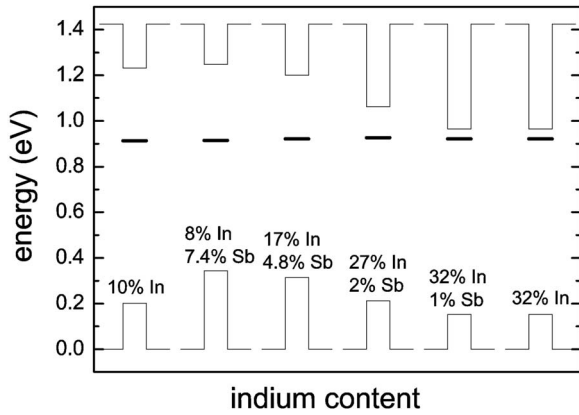


FIG. 3. Band gap lineup for the GaInNAs(Sb)/GaAs system with various In content together with the Fermi level position in the QW region.

with varying indium content (detailed contents are given in the figure caption). Two regions of optical transitions are visible for these samples. The first region, below 1.4 eV, is associated with optical transitions between energy levels confined in the GaInNAs(Sb)/GaAs QW. The second region, at 1.42 eV with strong FKOs, is associated with bulklike absorption inside the GaAs cap epilayer.¹⁰ In order to determine the Fermi level position in the QW region, both the band gap discontinuity at the GaInNAsSb/GaAs interface and the built-in electric field in the GaAs cap layer have to be known (see Fig. 1). The analysis of QW transitions allows us to determine the band gap discontinuity at the GaInNAs(Sb)/GaAs interface, whereas the analysis of FKOs allows us to determine the built-in electric field in the GaAs cap layer.¹⁰

A. Band gap discontinuity

The QW transitions were analyzed using the low-field electromodulation Lorentzian line shape functional form²³ (see details in Ref. 20). The dashed lines in Fig. 2 represent the modulus of individual CER resonances (individual QW transitions), and the notation $k/H(L)$ denotes the transition between the k th heavy-hole (light-hole) valence subband and the l th conduction subband. The identification of QW transitions was possible due to a series of calculations, which has been described in detail elsewhere.^{19,20} It has been found that the conduction band offset for this set of QWs increases from 40% to 80% with the increase in indium content from 8% to 32%.²⁰ Note that the change in indium content is combined with changes in the antimony content, and therefore the change in conduction band offset is not purely indium related. The band gap lineup for strained QWs is shown in Fig. 3. In addition, the band gap lineup for the Sb-free QWs is shown in this figure. The conduction band offset for the Sb-free QWs was investigated in Refs. 24 and 25.

B. Built-in electric field

Figure 4 shows CER spectra in the vicinity of GaAs-related absorption for GaInNAsSb/GaAs QW samples with varying indium content. At least eight clear FKO extrema are visible for the four samples. The extrema are given by²⁶

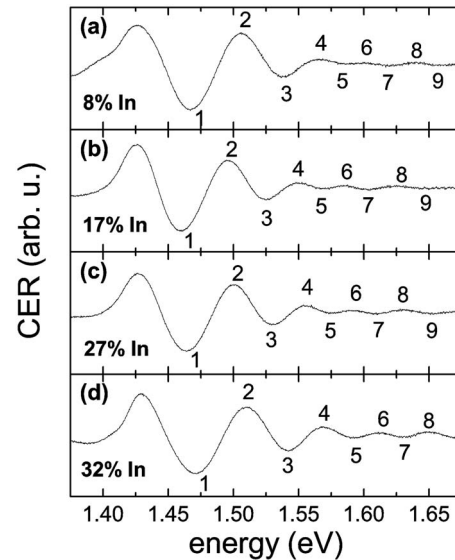


FIG. 4. Room temperature CER spectra for modified van Hoof structures with (a) Ga_{0.92}In_{0.08}N_{0.025}As_{0.901}Sb_{0.074}, (b) Ga_{0.83}In_{0.17}N_{0.025}As_{0.927}Sb_{0.048}, (c) Ga_{0.73}In_{0.27}N_{0.025}As_{0.955}Sb_{0.02}, and (d) Ga_{0.68}In_{0.32}N_{0.025}As_{0.965}Sb_{0.01} QWs.

$$n\pi = \varphi + \frac{4}{3} \left[\frac{(E_n - E_g)}{\hbar\theta} \right]^{3/2}, \quad (1)$$

where n is the index of the n th extrema, φ is an arbitrary phase factor, E_n is the energy of the n th extrema, and E_g is the energy gap. The electro-optic energy is given by

$$(\hbar\theta)^3 = \frac{e^2 \hbar^2 F^2}{2\mu}, \quad (2)$$

where μ is the reduced interband effective mass for the electron and heavy-hole pair in the direction of the electric field [for the (100) direction in GaAs the μ is $0.055m_0$ after Ref. 27]. A plot of $(4/3\pi)(E_n - E_g)^{3/2}$ versus n yields a straight line, with a slope proportional to the built-in electric field F . Appropriate plots for the four GaInNAsSb/GaAs QW samples and two GaInNAs/GaAs QW samples are shown in Fig. 5. It has been found that the slope yields electric fields

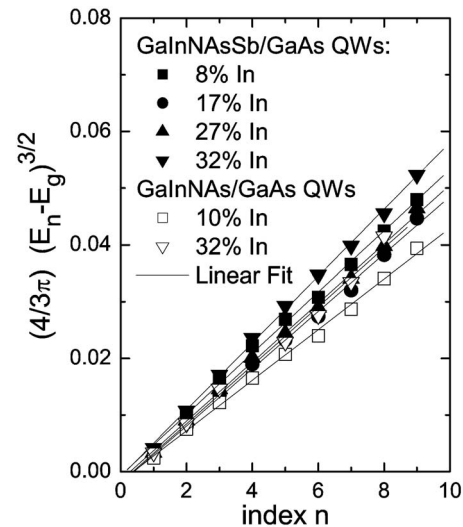


FIG. 5. Analysis of the period of GaAs-related FKOs.

of 67, 63, 65, and 73 kV/cm for the GaInNAsSb/GaAs QW sample with 8%, 17%, 27%, and 32% indium, respectively, and electric fields of 58 and 64 keV/cm for the GaInNAs/GaAs QW sample with 10% and 32% of In, respectively. In general, any strong changes in the electric field are not observed. For the Sb-free samples the electric field increases with the increase in indium content, but it is difficult to find this trend for Sb-containing QWs. However, it should be noted that the Sb concentration in GaInNAsSb/GaAs QWs changes from 7.4% to 1% when the indium content increased from 8% to 34%. Comparing Sb-free and Sb-containing QW samples with low indium content (full and open squares in Fig. 5), it has been found that the built-in electric field is higher after the Sb incorporation. It explains why no clear trend in the electric field is observed for GaInNAsSb/GaAs QWs. As will be concluded in Sec. III E, the value of the built-in electric field is correlated with the quality of the GaInNAs(Sb) layer.

C. Stark shift and band offset

The built-in electric field influences energies of QW transitions as well as the energy difference between electron (hole) levels. In order to investigate how the Stark effect is important for these structures, the three situations with various electric fields in the QW region have been considered for a $\text{Ga}_{0.83}\text{In}_{0.17}\text{N}_{0.025}\text{As}_{0.927}\text{Sb}_{0.048}/\text{GaAs}$ QW. It has been assumed that the internal electric field in this structure is the same as that in Fig. 1 and fulfills

$$\Phi = F_1 d_1 + F_2 d_2, \quad (3)$$

where Φ is the surface potential for GaAs [0.7 eV (Ref. 26)], F_1 and F_2 are the built-in electric fields in the GaAs cap and buffer layers, respectively, and d_1 and d_2 are the thicknesses of the GaAs cap and buffer layers, respectively. The built-in electric fields in the QW region are F_1 , F_2 , and $(F_1 + F_2)/2$ for situations (i), (ii), and (iii), respectively.

Figures 6(a) and 6(b) show the energy of 22H and 11H transitions, respectively, for the three situations as a function of the built-in electric field in the GaAs cap layer. The energy difference between 22H and 11H transitions is shown in Fig. 6(c). It is clearly visible that the Stark shift in the QW transitions and its influence on the energy difference between QW transitions are very small for 7.5 nm width GaInNAsSb QWs in this regime of electric fields. Note that situation (i) should be treated as a maximum estimation of the electric field in the QW region, whereas situation (ii) corresponds to a minimum estimation of this field. However, the real value of the electric field in the QW region can be even smaller than the minimum estimation of the electric field [i.e., situation (ii)] since the whole GaInNAs(Sb) region pins the Fermi level at a given energy, as will be concluded in Sec. III E, and a possible gradient of the Fermi level pinning in the QW area should be very small. Finally, it has been concluded that the Stark effect can be neglected during the analysis of the conduction band offset for these samples.

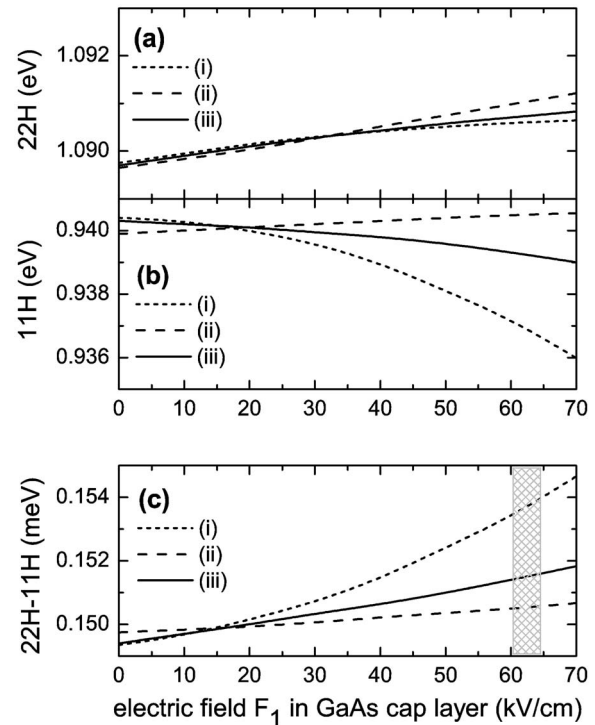


FIG. 6. Energies of 11H and 22H transitions for $\text{Ga}_{0.83}\text{In}_{0.17}\text{N}_{0.025}\text{As}_{0.927}\text{Sb}_{0.048}$ QW and the energy difference between them as a function of the built-in electric field in the GaAs cap layer. The built-in electric fields in the QW region are F_1 (short dashed lines), F_2 (dashed lines), and $(F_1 + F_2)/2$ (solid lines) for $F_1 = F_2 = 0$: $E_{11H} = 0.9405$ eV, $E_{22H} = 1.090$ eV, and $E_{22H-11H} = 149.5$ meV. The gray bar is plotted at the electric field, which was determined from the FKO period.

D. Fermi level position in GaInNAs(Sb)/GaAs quantum wells

The position of the Fermi level in the GaInNAs(Sb) QW region is calculated

$$\Delta E = \Phi - \Phi^* - \Delta E_C^*, \quad (4)$$

where $\Phi^* = Fd_1$ (see Fig. 1), ΔE_C^* is the band gap discontinuity in the strained QW, and ΔE is the energy difference between the Fermi level position and the conduction band minimum in the QW.

Figure 3 shows the Fermi level position in GaInNAs(Sb)/GaAs QWs plotted on the band gap diagram. This position with reference to the valence (conduction) band maximum in GaInNAs(Sb) increases (decreases) when the indium content increases. However, in an “absolute” energy scale, this position does not shift significantly and is located ~ 0.9 eV above the GaAs valence band maximum for all samples. It means that the Fermi level is pinned at a characteristic energy that is an intrinsic property of a given material. An interpretation of this energy applicable to the entire GaInNAs(Sb) composition range can be made in terms of Zunger’s^{28,29} “vacuum pinning rule” and/or Walukiewicz’s^{30–32} amphoteric native defect model. Walukiewicz^{30–32} proposed that for sufficiently high damage density, i.e., when the properties of the material are fully controlled by native defects, the Fermi energy stabilizes at a certain energy and becomes insensitive to further damage. The location of this Fermi level stabilization energy E_{FS} does

not depend on the type or the doping level of the original material and therefore is considered to be an intrinsic property of a given material. For GaAs this energy has been found $\sim 0.6\text{--}0.8$ eV above the valence band maximum,^{30–32} i.e., ~ 4.9 eV below the vacuum level. For other III-V semiconductors the E_{FS} was observed $\sim 4.9 \pm 0.2$ eV below the vacuum level.^{30–32} It is expected that for dilute nitrides the Fermi energy should also stabilize ~ 4.9 eV below the vacuum level. In the case of all GaInNAs(Sb) QWs the position of the Fermi level has been found 4.7 eV below the vacuum level. Therefore, we can conclude that the Fermi level in as-grown GaInNAsSb QWs is pinned very close to the Fermi level stabilization energy.

In general, the Fermi level stabilizes at E_{FS} for suitably high damage density. Ion bombardment³³ or other methods are used to achieve a high concentration of point defects in a given material. However, in the case of dilute nitrides, a high concentration of native point defect already exists for an as-grown material. These defects are associated with the incorporation of nitrogen into the III-V matrix. When the nitrogen concentration increases, the damage density in GaInNAs(Sb) increases as well. For samples studied in this paper, the nitrogen concentration in all samples is approximately constant ($\sim 2.5\%$), and therefore the point defect density should be comparable for all samples except the one that is Sb-free and has high indium content. However, the exact defect concentration in GaInNAs(Sb) is unknown because it is difficult to measure this quantity, especially for quinary alloys where many different native defects are possible. Moreover, it is well known that an appropriate experimental technique has to be used to measure individual defects; e.g., the positron annihilation is sensitive to neutral and negative vacancy-type defects,^{34,35} whereas other techniques are dedicated to other defects. In order to evaluate the degree of damage in the as-grown samples, a simple PL spectroscopy has been applied. This technique is sensitive to each kind of point defect if the defects have created nonradiative centers. PL spectra were measured in a standard experimental configuration, utilizing an argon ion laser as the excitation source. It has been observed that none of the as-grown samples emit light at room temperature for low excitation conditions (1 W/cm^2), whereas the annealed samples emit light even at lower excitation conditions. Light emission from the as-grown QW samples was observed at low temperatures, but it was a defect-related emission. To observe QW emission from as-grown samples at room temperature, the excitation density had to be increased to saturate the nonradiative recombination paths. Finally, the QW emission from as-grown samples was observed for excitation densities higher than 100 W/cm^2 . At this excitation condition, the QW emission from annealed samples was typically ten or more times stronger (see Ref. 36). These results confirm a significant concentration of native point defects inside the as-grown GaInNAsSb material. In general, it is possible that the degree of damage for GaInNAs(Sb) is insufficient to pin the Fermi level exactly at the E_{FS} , but surely the Fermi level is pinned close to the E_{FS} .

In the case of an annealed material, the concentration of native point defects decreases significantly and the Fermi

level can be unpinned or located at another energy different from E_{FS} . Such an effect has been observed for these samples since it has been found that the built-in electric field increases after annealing.³⁷ The increase in the built-in electric field in the GaAs cap layer can be explained by a shift in the Fermi level pinning in the GaInNAs(Sb) QW toward the conduction band and/or a shift in the Fermi level pinning at the GaAs surface toward the valence band. The shift in the Fermi level pinning at the GaAs surface has been found to be negligibly small for a reference sample, i.e., van Hoof structure without QW. Therefore the increase in the built-in electric field has been attributed to the Fermi level shift toward the conduction band in the GaInNAs(Sb) QW region.³⁷

Another important property of GaInNAs(Sb) alloy, which is observed in Fig. 3, is that the material becomes n type with the rise in indium composition. There is a general rule that semiconductor alloys with the conduction (valence) band located close to E_{FS} can be easily n -type (p -type) doped. To comply with this rule for GaInNAsSb alloys, it is expected that much higher electron concentrations can be achieved for GaInNAsSb alloys with high indium content than for alloys with low indium content. Moreover, for GaInNAsSb with high indium content, it could be difficult to achieve high-hole concentration since the E_{FS} is located close or inside the conduction band. In order to enhance susceptibility of GaInNAsSb to p -type doping, the antimony concentration has to be increased (compare the Sb-free and Sb-containing QWs in Fig. 3). According to the band anti-crossing model,¹ the N incorporation into this system pushes the conduction band to the E_{FS} and hence enhances the susceptibility of GaInNAsSb to n -type doping. Recently, it has been demonstrated that the incorporation of N into GaInAs increases the maximal electron concentration in this material.³⁸ Quinary GaInNAsSb alloys allow better control of the maximal electron (hole) concentration since indium atoms influence both the conduction and valence band discontinuities,²⁰ whereas nitrogen atoms influence mainly the conduction band,^{1,39} and antimony atoms influence mainly the valence band.^{19,24,40}

E. Fermi position and formation energy of native point defects in GaInNAs(Sb)

The Fermi level position is one of the parameters that influences the formation energy of native point defects in semiconductors.¹⁷ In general, it is expected that the Fermi level in undoped semiconductors is located close to the middle of the energy gap. In fact, the Fermi level can be shifted to the conduction (or valence) band because of native point defects and background impurities, which always exist in real semiconductor materials; the background concentration of point defects influences the formation energy of these defects and vice versa. This mechanism is complex since different point defects are involved in this process; the formation energy for each of point defects is different, and its dependence on the Fermi energy is different.¹⁷ Typically, point defects, which generate multiple-charged deep states, are able to pin the Fermi level at the E_{FS} . In the case of dilute nitrides, the exact nature of native point defects is still unknown especially for quaternary or quinary alloys. However,

the observation that the Fermi level is pinned close to the E_{FS} for all GaInNAs(Sb)/GaAs QW samples suggests that the concentration of multiple-charged deep states is significant for the as-grown material.

As seen in Fig. 3, the energy difference between the Fermi level position and the conduction band decreases when the In content increases. According to Ref. 17, it can be also assumed that the formation energy of some point defects in GaInNAs(Sb) should be much smaller when the Fermi level is located close to the conduction band. With some growth conditions, the native point defects can form spontaneously and lead to phase separation in this material since the energy formation of these defects can be very low. An investigation of the Fermi level position in GaInNAs(Sb) alloys shows that this scenario is very probable for In-rich (In > 32%) dilute nitrides since in these materials the Fermi level is pinned at the conduction band. This scenario is also very probable for InNAs alloys and can explain difficulties with the growth of good quality InNAs material.

IV. CONCLUSIONS

In conclusion, the Fermi level position in as-grown GaInNAs(Sb)/GaAs QWs has been investigated using CER spectroscopy. It has been observed that the Fermi level is pinned for all samples at the same energy in an absolute scale. This energy is located ~ 4.7 eV below the vacuum level and hence is attributed to the Fermi level stabilization energy, which is known to be ~ 4.9 eV for all semiconductor materials. It has been concluded that the reason for Fermi level pinning in GaInNAs(Sb) at this energy is a high concentration of native point defect in the as-grown material. Due to the significant differences between the electronegativity and size of atoms in this material system, large numbers of native point defects appear more easily than in common semiconductor alloys (e.g., GaInAs). Thus the effect of Fermi level pinning close to the Fermi level stabilization energy in an as-grown material can be typical for the class of highly mismatched semiconductor alloys.

ACKNOWLEDGMENTS

We acknowledge the support from the Foundation for Polish Science through Subsidy 8/2005, the Defense Advanced Research Projects Agency (DARPA) and the Army Research Office (ARO) (Contract Nos. MDA972-00-1-024, DAAD17-02-C-0101, and DAAD199-02-1-0184), the Office of Naval Research (ONR) (Contract No. N00014-01-1-00100), the MNiSW (Grant No. N515 074 31/3896), as well as the Stanford Network Research Center. R.K. acknowledges support from the Foundation for Polish Science. H.Y. acknowledges support from the Stanford Graduate Fellowships.

¹W. Shan, W. Walukiewicz, J. W. Ager III, E. E. Haller, J. F. Geisz, D. J. Friedman, J. M. Olson, and S. R. Krutz, *Phys. Rev. Lett.* **82**, 1221 (1999).

²T. Mattila, S. H. Wei, and A. Zunger, *Phys. Rev. B* **60**, R11245 (1999).

³N. G. Szewski and P. Boguslawski, *Phys. Rev. B* **64**, 161201 (2001).

⁴J. Wu, W. Walukiewicz, and E. E. Haller, *Phys. Rev. B* **65**, 233210 (2002).

⁵A. Lindsay and E. P. O'Reilly, *Phys. Rev. Lett.* **93**, 196402 (2004).

⁶M. Weyers, M. Sato, and H. Ando, *Jpn. J. Appl. Phys., Part 2* **31**, L853 (1992).

⁷C. Skierbiszewski, P. Perlin, P. Wisniewski, W. Knap, T. Suski, W. Walukiewicz, W. Shan, K. M. Yu, J. W. Ager, E. E. Haller, J. F. Geisz, and J. M. Olson, *Appl. Phys. Lett.* **76**, 2409 (2000).

⁸P. N. Hai, W. M. Chen, I. A. Buyanova, H. P. Xin, and C. W. Tu, *Appl. Phys. Lett.* **77**, 1843 (2000).

⁹See, for example, M. Henini, *Dilute Nitride Semiconductors* (Elsevier, Oxford, 2005).

¹⁰R. Kudrawiec, H. B. Yuen, S. R. Bank, H. P. Bae, M. A. Wistey, J. S. Harris, M. Motyka, and J. Misiewicz, *J. Appl. Phys.* **102**, 113501 (2007).

¹¹X. Kong, A. Trampert, E. Tournie, and K. H. Ploog, *Appl. Phys. Lett.* **87**, 171901 (2005).

¹²H. Y. Liu, C. M. Tey, C. Y. Jin, S. L. Liew, P. Navaretti, M. Hopkinson, and A. G. Cullis, *Appl. Phys. Lett.* **88**, 191907 (2006).

¹³J. S. Harris, Jr., *J. Cryst. Growth* **278**, 3 (2005), and references therein.

¹⁴H. B. Yuen, S. R. Bank, H. Bae, M. A. Wistey, and J. S. Harris, Jr., *J. Appl. Phys.* **99**, 093504 (2006).

¹⁵J. S. Harris, Jr., R. Kudrawiec, H. B. Yuen, S. R. Bank, H. P. Bae, M. A. Wistey, D. Jackrel, E. R. Pickett, T. Sarmiento, L. L. Goddard, V. Lordi, and T. Gugov, *Phys. Status Solidi A* **244**, 2707 (2007).

¹⁶S. R. Bank, H. Bae, L. L. Goddard, H. B. Yuen, M. A. Wistey, R. Kudrawiec, and J. S. Harris, *IEEE J. Quantum Electron.* **43**, 773 (2007).

¹⁷C. G. Van de Walle and J. Neugebauer, *J. Appl. Phys.* **95**, 3851 (2004).

¹⁸R. Kudrawiec and J. Misiewicz, *Appl. Surf. Sci.* **253**, 80 (2006).

¹⁹R. Kudrawiec, M. Gladysiewicz, J. Misiewicz, H. B. Yuen, S. R. Bank, M. A. Wistey, H. P. Bae, and J. S. Harris, Jr., *Phys. Rev. B* **73**, 245413 (2006).

²⁰R. Kudrawiec, H. B. Yuen, M. Motyka, M. Gladysiewicz, J. Misiewicz, S. R. Bank, H. P. Bae, M. A. Wistey, and J. S. Harris, *J. Appl. Phys.* **101**, 013504 (2007).

²¹M. Motyka, R. Kudrawiec, and J. Misiewicz, *Phys. Status Solidi A* **204**, 354 (2007).

²²J. Misiewicz, P. Sitarek, G. Sek, and R. Kudrawiec, *Mater. Sci.* **21**, 263 (2003).

²³D. E. Aspnes, *Surf. Sci.* **37**, 418 (1973).

²⁴R. Kudrawiec, M. Motyka, M. Gladysiewicz, J. Misiewicz, H. B. Yuen, S. R. Bank, H. Bae, M. A. Wistey, and J. S. Harris, *Appl. Phys. Lett.* **88**, 221113 (2006).

²⁵R. Kudrawiec, H. B. Yuen, S. R. Bank, H. Bae, M. A. Wistey, J. S. Harris, M. Motyka, M. Gladysiewicz, and J. Misiewicz, *Phys. Status Solidi A* **204**, 364 (2007).

²⁶H. Shen and M. Dutta, *J. Appl. Phys.* **78**, 2151 (1995), and references therein.

²⁷I. Vurgaftman and J. R. Meyer, *J. Appl. Phys.* **94**, 3675 (2003).

²⁸Z. Zunger, *Phys. Rev. Lett.* **54**, 849 (1985).

²⁹M. J. Celdas, A. Fazio, and A. Zunger, *Appl. Phys. Lett.* **45**, 671 (1984).

³⁰W. Walukiewicz, *J. Vac. Sci. Technol. B* **6**, 1257 (1988).

³¹W. Walukiewicz, *Phys. Rev. B* **37**, 4760 (1988).

³²W. Walukiewicz, *Physica B (Amsterdam)* **302–303**, 123 (2001).

³³S. X. Li, K. M. Yu, J. Wu, R. E. Jones, W. Walukiewicz, J. W. Ager III, W. Shan, E. E. Haller, H. Lu, and W. J. Schaff, *Phys. Rev. B* **71**, 161201(R) (2005).

³⁴J. Toivonen, T. Hakkarainen, M. Sopenan, H. Lipsanen, J. Oila, and K. Saarinen, *Appl. Phys. Lett.* **82**, 40 (2003).

³⁵A. J. Ptak, S. Kurtz, M. H. Weber, and K. G. Lynn, *J. Vac. Sci. Technol. B* **22**, 1584 (2004).

³⁶H. B. Yuen, S. R. Bank, H. Bae, M. A. Wistey, and J. S. Harris, Jr., *Appl. Phys. Lett.* **88**, 221913 (2006).

³⁷R. Kudrawiec, H. B. Yuen, S. R. Bank, H. P. Bae, M. A. Wistey, J. S. Harris, M. Motyka, and J. Misiewicz, *Appl. Phys. Lett.* **90**, 061902 (2007).

³⁸K. M. Yu, W. Walukiewicz, W. Shan, J. W. Ager III, J. Wu, E. E. Haller, J. F. Geisz, D. J. Friedman, and J. M. Olson, *Phys. Rev. B* **61**, R13337 (2000).

³⁹R. Kudrawiec, M. Motyka, M. Gladysiewicz, J. Misiewicz, J. A. Gupta, and G. C. Aers, *Solid State Commun.* **138**, 365 (2006).

⁴⁰R. Kudrawiec, J. A. Gupta, M. Motyka, M. Gladysiewicz, J. Misiewicz, and X. Wu, *Appl. Phys. Lett.* **89**, 171914 (2006).